



Original Article

Honokiol enhances temozolomide-induced apoptotic insults to malignant glioma cells via an intrinsic mitochondrion-dependent pathway

Chung-Ching Chio^{a,b,1}, Yu-Ting Tai^{c,1}, Mahendrarman Mohanraj^b, Shing-Hwa Liu^d,
Shun-Tai Yang^e, Ruei-Ming Chen^{b,f,g,*}



^a Department of Neurosurgery, Chi-Mei Medical Center, Tainan, Taiwan

^b Graduate Institute of Medical Sciences, College of Medicine, Research Center of Cancer Translational Medicine, Taipei Medical University, Taipei, Taiwan

^c Department of Anesthesiology, Wan-Fang Hospital, Taipei Medical University, Taipei, Taiwan

^d Institute of Toxicology, College of Medicine, National Taiwan University, Taipei, Taiwan

^e Department of Neurosurgery, Shuang-Ho Hospital, Taipei Medical University, New Taipei City, Taiwan

^f Anesthesiology and Health Policy Research Center, Taipei Medical University Hospital, Taipei, Taiwan

^g Brain Disease Research Center, Wan-Fang Hospital, Taipei Medical University, Taipei, Taiwan

ARTICLE INFO

Keywords:

Malignant glioma
Honokiol
Temozolomide
Apoptosis
Intrinsic pathway

ABSTRACT

Background: Temozolomide (TMZ) is a first-line chemotherapeutic drug for malignant gliomas. Nonetheless, TMZ-induced side effects and drug resistance remain challenges. Our previous study showed the suppressive effects of honokiol on growth of gliomas.

Purpose: This study was further aimed to evaluate if honokiol could enhance TMZ-induced insults toward malignant glioma cells and its possible mechanisms.

Methods: Human U87 MG glioma cells were exposed to TMZ, honokiol, and a combination of TMZ and honokiol. Cell survival, apoptosis, necrosis, and proliferation were successively assayed. Fluorometric substrate assays were conducted to determine activities of caspase-3, -6, -8, and -9. Levels of Fas ligand, Bax, and cytochrome c were immunodetected. Translocation of Bax to mitochondria were examined using confocal microscopy. Mitochondrial function was evaluated by assaying the mitochondrial membrane potential (MMP), reactive oxygen species (ROS), and complex I enzyme activity. Caspase-6 activity was suppressed using specific peptide inhibitors. The honokiol-induced effects were further confirmed using human U373 MG and murine GL261 cells.

Results: Exposure of human U87 MG glioma cells to honokiol significantly increased TMZ-induced DNA fragmentation and cell apoptosis. Interestingly, honokiol enhanced intrinsic caspase-9 activity without affecting extrinsic Fas ligand levels and caspase-8 activity. Sequentially, TMZ-induced changes in Bax translocation, the MMP, mitochondrial complex I enzyme activity, intracellular ROS levels, and cytochrome c release were enhanced by honokiol. Consequently, honokiol amplified TMZ-induced activation of caspases-3 and -6 in human U87 MG cells. Fascinatingly, suppressing caspase-6 activity concurrently decreased honokiol-induced DNA fragmentation and cell apoptosis. The honokiol-involved improvement in TMZ-induced intrinsic apoptosis was also confirmed in human U373 MG and murine GL261 glioma cells.

Conclusions: This study showed that honokiol can enhance TMZ-induced apoptotic insults to glioma cells via an intrinsic mitochondrion-dependent mechanism. Our results suggest the therapeutic potential of honokiol to attenuate TMZ-induced side effects.

Abbreviations: ANOVA, analysis of variance; Bax, Bcl-2-associated X protein; BrdU, bromodeoxyuridine; CI, combination index; DEVD, Asp-Glu-Val-Asp; DiOC₆, 3,3'-dihexyloxycarbocyanine; DAPI, 4'-6-diamidino-2-phenylindole; DMEM, Dulbecco's modified Eagle's medium; DMSO, dimethyl sulfoxide; EDTA, ethylenediaminetetraacetic acid; ELISA, enzyme-linked immunosorbent assay; FBS, fetal bovine serum; GAPDH, glyceraldehyde 3-phosphate dehydrogenase; HEPES, 25 mM 4-(2-hydroxyethyl)-1-piperazineethanesulfonic acid; IETD, Ile-Glu-Thr-Asp; LEHD, Leu-Glu-His-Asp; mAb, monoclonal antibody; MMP, mitochondrial membrane potential; PAGE, polyacrylamide gel electrophoresis; PBS, phosphate-buffered saline; ROS, reactive oxygen species; SDS, sodium dodecylsulfate; VEID, Val-Glu-Ile-Asp

* Corresponding author at: Graduate Institute of Medical Sciences, College of Medicine, Taipei Medical University, 250 Wu-Xing St., Taipei 11031, Taiwan.

E-mail address: rmchen@tmu.edu.tw (R.-M. Chen).

¹ Chung-Ching Chio and Yu-Ting Tai equally contribute to this scientific work.

<https://doi.org/10.1016/j.phymed.2018.06.012>

Received 8 February 2018; Received in revised form 24 May 2018; Accepted 11 June 2018

0944-7113/© 2018 Elsevier GmbH. All rights reserved.

Introduction

Brain tumors comprise primary tumors of the central nervous system and secondary metastatic tumors (Seano, 2018). Gliomas that predominantly arise from transformation of astrocytes, oligodendrocytes, and ependymal cells are the most common brain tumors (Saadatpour et al., 2016; Seano, 2018). According to a grading system of the World Health Organization, gliomas are classed into low- (grades I and II) and high- (grades III and IV) grade tumors. Glioblastoma multiforme (GBM), classified as a high-grade (grade IV) glioma, is the most aggressive brain tumor. In the clinic, the recommended therapy for GBM patients is surgical resection followed by irradiation and adjuvant chemotherapy, but the median overall survival time of GBM patients is only about 12 months (Daher and de Groot, 2018). The poor outcomes are due to uncontrolled tumor proliferation, infiltrative growth, angiogenesis, and resistance to apoptosis (Furnari et al., 2015). Temozolomide (TMZ), a DNA-alkylating agent, is the chief chemotherapeutic drug for treating GBM patients (Hottinger et al., 2016). TMZ can freely pass through the blood-brain barrier (BBB) and subsequently induces apoptosis of glioma cells by alkylating guanine at the O⁶ site (Hottinger et al., 2016; Seano, 2018). Unfortunately, TMZ can lead to various side effects, such as nausea, vomiting, constipation, headaches, fatigue, loss of appetite, mouth sores, and hair loss, as well as drug resistance (Omuro and DeAngelis, 2013). These complications reduce therapeutic effects of TMZ and quality of life of GBM patients. As a result, discovering new drugs that can improve TMZ's capacity while reducing its side effects is urgent and necessary.

Honokiol (2-(4-hydroxy-3-prop-2-enyl-phenyl)-4-prop-2-enyl-phenol), one of the main physiologically bioactive constituents of the traditional Chinese medicine Houpo (*Magnolia officinalis* Rehd. et Wils.), exhibits diverse anti-inflammatory, antimicrobial, antithrombotic, and anxiolytic effects (Hahm et al., 2008; Pan et al., 2016). Previous studies showed that honokiol can be used for treating diverse diseases such as anxiety, nervous disturbances, thrombotic stroke, typhoid fever, and dead muscles (Lo et al., 1994; Fried and Arbiser, 2009). Moreover, honokiol possesses antitumor activities against leukemia, breast cancer, pancreatic cancer, and oral squamous cell carcinoma cells due to induction of cell cycle arrest and cell apoptosis (Bonner et al., 2016; Bilia et al., 2017). We conducted consecutive studies in our lab on antitumor activities of honokiol against brain tumors. At first, we demonstrated that honokiol can pass through the BBB *in vitro* and *in vivo* (Lin et al., 2012). Then, we showed the safety of honokiol to brain normal cells and its ability to kill neuroblastoma cells and glioma cells via an apoptotic mechanism (Lin et al., 2016a,b). Furthermore, we reported the autophagic effects of honokiol on glioma cells and neuroblastoma cells (Lin et al., 2016b; Yeh et al., 2016). Recently, we demonstrated that honokiol can kill drug-sensitive and -resistant glioma cells (Chio et al., 2018). Therefore, honokiol may have the potential to be clinically applied for combined treatment with TMZ in order to reduce its side effects and drug resistance.

Apoptosis, a process of programmed cell death, is characterized by distinct morphological characteristics and energy-dependent biochemical mechanisms (Aubrey et al., 2018). When discovering *de novo* drugs for cancer therapy, we generally design such drug candidates so that they can specifically induce apoptosis of tumor cells (Mills et al., 2018). A variety of intrinsic and extrinsic factors contribute to cell apoptosis (Goyal, 2001). The extrinsic apoptosis pathway is initiated following binding of death Fas ligand to death Fas receptor, contributing to activation of caspase-8 (Bao and Shi, 2007). In contrast, caspase-9 is activated via an intrinsic mitochondrion-dependent pathway (Bao and Shi, 2007; Chen et al., 2013). In an intrinsic apoptotic mechanism, translocation of proapoptotic Bax protein from the cytoplasm to mitochondria can permeabilize the outer membrane, which then disturbs the mitochondrial membrane potential (MMP) and triggers release of cytochrome *c* and reactive oxygen species (ROS) (Franklin, 2011;

Chang et al., 2016). Afterward, cytochrome *c* can stimulate cascade activation of caspases-9, -3, and -6 that can cleave key cellular proteins and consequently fragment genomic DNA (Goyal, 2001). Our previous studies showed that honokiol can induce apoptotic insults to neuroblastoma and glioma cells via an intrinsic pathway. Recently, we reported the effects of hypoxia-induced autophagic death for treating human malignant glioma cells (Cheng et al., 2017). Furthermore, we also demonstrated the capacity of honokiol to induce autophagic apoptosis in brain tumor cells (Lin et al., 2016b; Yeh et al., 2016). Thus, this study was aimed to further verify if honokiol could enhance TMZ-induced insults to malignant glioma cells and its possible mechanisms.

Materials and methods

Cell culture and drug treatment

The human glioma U87 MG and U373 MG cell lines were purchased from American Type Culture Collection (Manassas, VA, USA). Murine GL261 glioma cells were a kind gift from Dr. Rong-Tsun Wu (Institute of Biopharmaceutical Sciences, National Yang-Ming University, Taipei, Taiwan). Glioma cells were maintained in Dulbecco's modified Eagle's medium (DMEM, Gibco-BRL, Grand Island, NY, USA) supplemented with 10% fetal bovine serum, 2 mM L-glutamine, 100 IU/ml penicillin, 100 mg/ml streptomycin, 1 mM sodium pyruvate, and 1 mM non-essential amino acids at 37 °C in a humidified atmosphere of 5% CO₂. Cells were grown to confluence before drug treatment.

Honokiol and TMZ were purchased from Sigma (St. Louis, MO, USA) and freshly dissolved in dimethyl sulfoxide (DMSO). The purities of honokiol and TMZ used in this study were >98%. Cells were exposed to honokiol, TMZ, and a combination of honokiol and TMZ at different concentrations for various time intervals.

Cell morphology and cell survival assays

Cell survival was assayed using a trypan blue exclusion method as described previously (Lin et al., 2018). Glioma cells (2×10^4 cells) were seeded in 24-well tissue culture plates. After drug treatment, morphologies of glioma cells were observed and photographed (Nikon, Tokyo, Japan). Then, cells were trypsinized with 0.1% trypsin-EDTA (Gibco-BRL). Following centrifugation and washing, glioma cells were suspended in phosphate-buffered saline (PBS), containing 0.14 M NaCl, 2.6 mM KCl, 8 mM Na₂HPO₄, and 1.5 mM KH₂PO₄, and stained with trypan blue dye (Sigma). Fractions of dead cells with a blue signal were visualized and counted using a reverse-phase microscope (Nikon).

Quantification of DNA fragmentation

DNA fragmentation in glioma cells was quantified using a cellular DNA fragmentation enzyme-linked immunosorbent assay (ELISA) kit (Boehringer Mannheim, Indianapolis, IN, USA) as described previously (Chuang et al., 2011). Briefly, glioma cells (2×10^5 cells) were seeded in 24-well tissue culture plates and labeled with bromodeoxyuridine (BrdU) overnight. Cells were harvested and suspended in DMEM. One hundred microliters of a cell suspension was added to each well of 96-well tissue culture plates. Glioma cells were treated with TMZ, honokiol, and a combination of honokiol and TMZ for different time intervals at 37 °C in a humidified atmosphere of 5% CO₂. Amounts of BrdU-labeled DNA in the cytoplasm were quantified using a microplate photometer (Anthos Labtec Instruments, Lagerhausstrasse, Wals/Salzburg, Austria).

Measurement of apoptotic cells

Apoptotic cells were determined by detecting cells which were arrested at the sub-G₁ stage as described previously (Chio et al., 2013).

After drug treatment, harvested glioma cells were fixed in cold 80% ethanol, then incubated with 3.75 mM sodium citrate, 0.1% Triton X-100, and 30 µg/ml RNase A, and resuspended in 20 µg/ml propidium iodide. Stained nuclei were analyzed by flow cytometry (Beckman Coulter, Fullerton, CA, USA).

Quantification of necrotic cells

Necrotic cells were quantified using a photometric immunoassay according to the standard protocol of the cell death detection kit (Roche Applied Sciences, Nonnenwald, Penzberg, Germany) as described previously (Chuang et al., 2011). Briefly, glioma cells (10^5 cells) were subcultured in 96-well tissue culture plates overnight. After drug treatment, cell lysates and culture medium were collected, and necrotic cells were immunodetected using mouse monoclonal antibodies (mAbs) against histone. After the antibody reaction and washing, the colorimetric product was measured at 405 nm against the substrate solution as a blank.

Analysis of cell proliferation

Proliferation of glioma cells was analyzed by measuring the incorporation of BrdU into genomic DNA as described previously (Ho et al., 2014). Glioma cells were seeded at 3×10^3 cells/well in 96-well microtiter plates. After drug treatment, 10 mM BrdU was added to the culture medium for incorporation into the DNA of replicating cells. After 2 h of incubation, cells were fixed in 4% paraformaldehyde. BrdU incorporation was determined by a cell proliferation ELISA BrdU kit (Roche, Mannheim, Germany).

Assay of caspase activities

Activities of caspases-3, -6, -8, and -9 were assayed using fluorometric assay kits (R&D Systems, Minneapolis, MN, USA) as described previously (Lin et al., 2016a; Wu et al., 2017). Briefly, after drug treatment, glioma cells were lysed using buffer containing 1% Nonidet P-40, 200 mM NaCl, 20 mM Tris/HCl (pH 7.4), 10 mg/ml leupeptin, 0.27 U/ml aprotinin, and 100 mM phenylmethanesulfonyl fluoride (PMSF). Cell extracts (25 mg total protein) were incubated with 50 mM of specific fluorogenic peptide substrates in 200 µl of a cell-free system buffer comprising 10 mM HEPES (pH 7.4), 220 mM mannitol, 68 mM sucrose, 2 mM NaCl, 2.5 mM KH_2PO_4 , 0.5 mM EGTA, 2 mM MgCl_2 , 5 mM pyruvate, 0.1 mM PMSF, and 1 mM dithiothreitol. Peptide substrates for assays of caspase-3, -6, -8, and -9 activities were Asp-Glu-Val-Asp (DEVD), Val-Glu-Ile-Asp (VEID), Ile-Glu-Thr-Asp (IETD) and Leu-Glu-His-Asp (LEHD), respectively. These peptides were conjugated to 7-amino-4-trifluoromethyl coumarin for fluorescence detection. For the inhibition assay, glioma cells were pretreated with 50 mM Z-VEID-FMK, an inhibitor of caspase-6, for 1 h, and then exposed to TMZ, honokiol, and their combination. Intensities of the fluorescent products were measured using an LS 55 spectrometer of PerkinElmer Instruments (Shelton, CT, USA).

Analysis of Bax translocation

Bax translocation in glioma cells was analyzed using confocal microscopy as described previously (Wu et al., 2016). Briefly, after drug treatment, glioma cells were fixed with a fixing reagent (acetone: methanol, 1:1) for 10 min. Following rehydration, cells were incubated with 0.2% Triton X-100 at room temperature for 15 min. The mouse mAb used in this study was generated against human Bax (Santa Cruz Biotechnology, Santa Cruz, CA, USA). Immunodetection of Bax in glioma cells was performed overnight. After washing, cells were sequentially reacted with second antibodies and biotin-SP-conjugated AffiniPure goat anti-rabbit immunoglobulin G (IgG; Jackson ImmunoResearch, West Grove, PA, USA) at room

temperature for 1 h. After washing, a third antibody with Cy3-conjugated streptavidin (Jackson ImmunoResearch) was added to glioma cells and reacted at room temperature for 30 min. Mitochondria and nuclei of fixed neuroblastoma cells were stained with 3,3'-dihexyloxycarbocyanine (DiOC₆; Molecular Probes, Eugene, OR, USA), a positively charged dye, and 4',6'-diamidino-2-phenylindole (DAPI). A confocal laser scanning microscope (model FV500, Olympus, Tokyo, Japan) was used for sample observation. Illumination of the existence of the Bax protein was demonstrated by the appearance of hot spots in both the cytoplasm (red signals) and membranes (yellow signals). Images were acquired and quantified using FluoView software (Olympus).

Immunoblot analyses

After drug treatment, glioma cells were washed with PBS and lysed with ice-cold lysis buffer (25 mM 4-(2-hydroxyethyl)-1-piperazineethanesulfonic acid (HEPES), 1.5% Triton X-100, 0.1% sodium dodecylsulfate (SDS), 0.5 M NaCl, 5 mM ethylenediaminetetraacetic acid (EDTA), and 0.1 mM sodium deoxycholate) containing a protease inhibitor cocktail. Protein concentrations were quantified using a bicinchoninic acid protein assay kit (Thermo, San Jose, CA, USA). An equal amount of proteins from each group was separated using SDS-polyacrylamide gel electrophoresis (PAGE), followed by transfer to nitrocellulose membranes. Membranes were incubated in a 5% skim milk solution for 1 h. Bax and cytochrome c were detected using a mouse mAb (Cell Signaling Technology, Danvers, MA, USA). Levels of Fas ligand were immunodetected using a goat polyclonal antibody against human Fas (GeneTex, Zeeland, MI, USA). Glyceraldehyde 3-phosphate dehydrogenase (GAPDH) was analyzed as an internal control. Membranes were probed with the appropriate horseradish peroxidase-conjugated secondary antibodies for 1 h at room temperature. Immunoreactive proteins were detected using an enhanced chemiluminescence reagent (PerkinElmer, Waltham MA, USA) and then imaged using a digital analyzer (Syngene, Cambridge, UK) and densitometry software (Syngene) as described previously (Chio et al., 2016).

Analysis of the MMP

The MMP of glioma cells was determined according to a previous method (Lin et al., 2012). Briefly, glioma cells (5×10^5 cells) were seeded in 12-well tissue culture plates overnight, and then treated with drugs. After drug administration, cells were harvested and incubated with DiOC₆, an intracellular green-fluorescent probe specifically used to detect the MMP of live cells, at 37 °C for 30 min in a humidified atmosphere of 5% CO₂. After washing and centrifugation, cell pellets were suspended in PBS. Intracellular fluorescent intensities were analyzed with a flow cytometer (Beckman Coulter).

Quantification of intracellular ROS

Levels of intracellular ROS in glioma cells were quantified following a previously described method (Chuang et al., 2011). Briefly, glioma cells (10^5 cells) were seeded in 12-well tissue culture plates overnight. Cells were co-treated with different drugs and with 2',7'-dichlorofluorescein diacetate, an ROS-sensitive dye. After drug treatment, glioma cells were harvested and suspended in PBS. Relative fluorescence intensities in glioma cells were quantified with a flow cytometer (Beckman Coulter).

Assay of the enzyme activity of mitochondrial complex I

Activity of the mitochondrial complex I enzyme was assayed using a colorimetric method as described previously (Lin et al., 2018). After drug administration, glioma cells were cultured with new medium

containing 0.5 mg/ml 3-(4,5-dimethylthiazol-2-yl)-2,5-diphenyltetrazolium bromide for a further 3 h. Blue formazan products in the osteoblasts were dissolved in DMSO and spectrophotometrically measured at a wavelength of 550 nm.

Statistical analysis

The statistical significance of differences between control and drug-treated groups was evaluated using Student's *t*-test, and differences were considered statistically significant at $p < 0.05$. Differences between drug-treated groups were considered significant when the *p* value of Duncan's multiple-range test was < 0.05 . Statistical analyses between groups over time were carried out by a two-way analysis of variance (ANOVA). In order to determine the drug interaction between TMZ and honokiol in killing human glioma cells, the combination index (CI) was calculated following a previously described method (Ooko et al., 2017).

Results

Honokiol improves TMZ-induced insults to human malignant glioma cells

Exposure of human U87 MG cells to 20, 40, 60, 80, and 100 μM honokiol for 72 h led to shrunken morphologies and decreased cell

numbers in a concentration-dependent manner (Fig. 1A). The half lethal concentration (LC_{50}) of honokiol was 62.52 μM (Fig. 1B). The CI index, indicating the interaction between TMZ and honokiol in killing human glioma cells, is equal to 0.956. Treatment of human U87 MG cells with 100 μM TMZ and 40 μM honokiol caused time-dependent reductions in cell survival (Fig. 1C). Compared to the TMZ-treated group, administration of honokiol led to an enhancement in TMZ-induced death of human malignant glioma cells. Exposure of human U87 MG cells to 40 μM honokiol for 72 h decreased cell survival by 30% (Fig. 1D). Cotreatment with honokiol and 25 μM TMZ did not affect honokiol-induced cell death. In contrast, when the concentrations reached 50, 75, and 100 μM , TMZ enhanced honokiol-induced death of human glioma cells by 28% ($p = 0.003$), 44% ($p = 0.002$), and 56% ($p = 0.002$), respectively (Fig. 1D).

Honokiol enhances TMZ-induced apoptosis and suppression of proliferation in human glioma cells

Exposure of human U87 MG cells to TMZ and honokiol alone for 72 h led to significant 89% and 70% increases in DNA fragmentation, respectively (Fig. 2A). In comparison, cotreatment with honokiol and TMZ elevated TMZ-induced DNA fragmentation by 56% ($p = 0.007$). Treatment of human U87 MG cells with TMZ and honokiol for 72 h triggered 39% and 35% of cells to undergo apoptosis, respectively

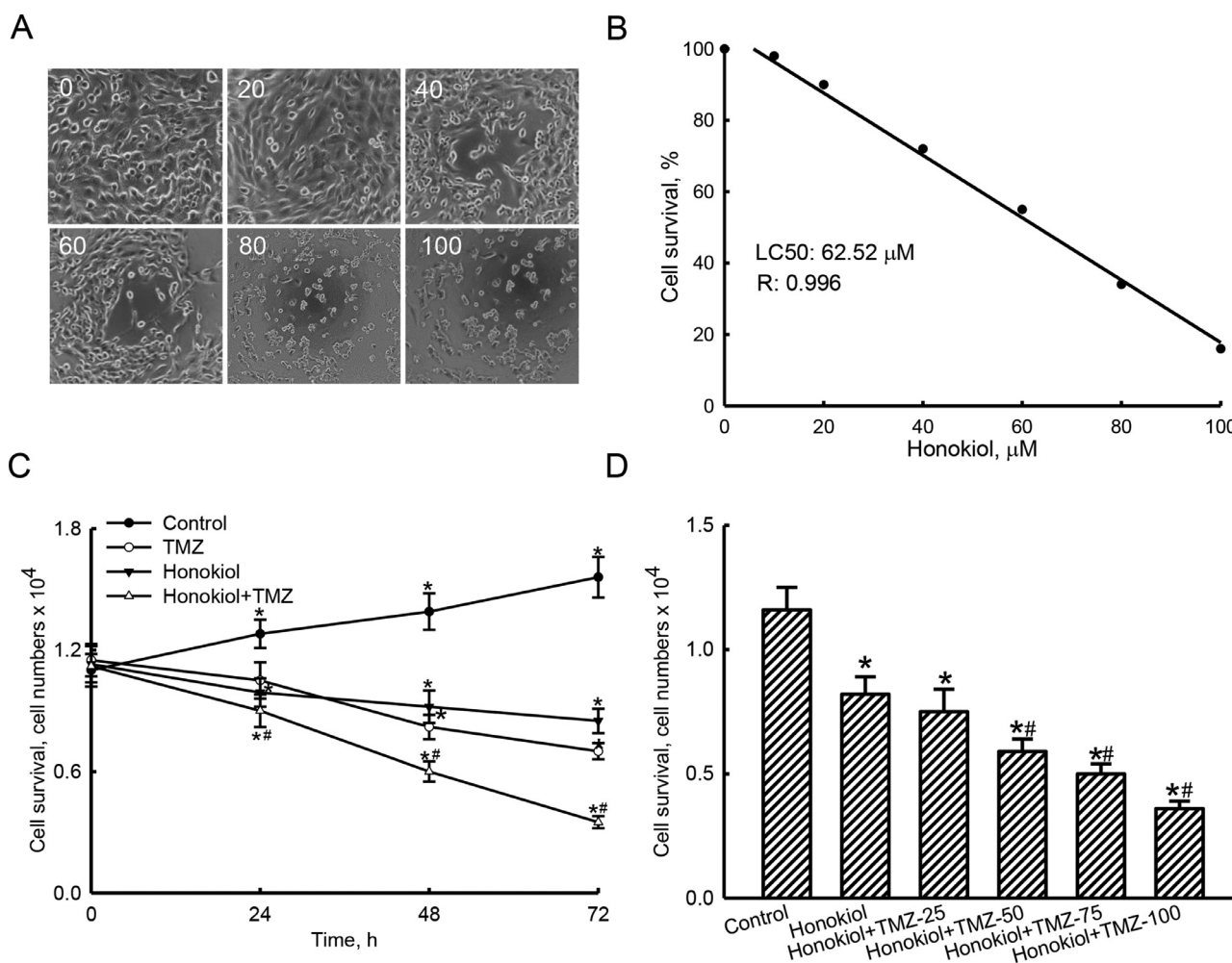


Fig. 1. Effects of honokiol on temozolomide (TMZ)-induced death of human glioma cells. Human U87 MG cells were exposed to 20, 40, 60, 80, and 100 μM honokiol for 72 h. Cell morphologies were observed and photographed (A). Cell survival was assessed with a trypan blue exclusion method (B). Human U87 MG cells were exposed to 100 μM TMZ, 40 μM honokiol, and their combination for 72 h, and cell survival was assayed (C). Human U87 MG cells were co-treated with 40 μM honokiol and 25, 50, 75, and 100 μM TMZ for 72 h. Cell survival was evaluated using a trypan blue exclusion method (D). Each value represents the mean \pm SEM for $n = 6$. Symbols * and # indicate that the values significantly ($p < 0.05$) differed from the control and honokiol-treated groups, respectively.

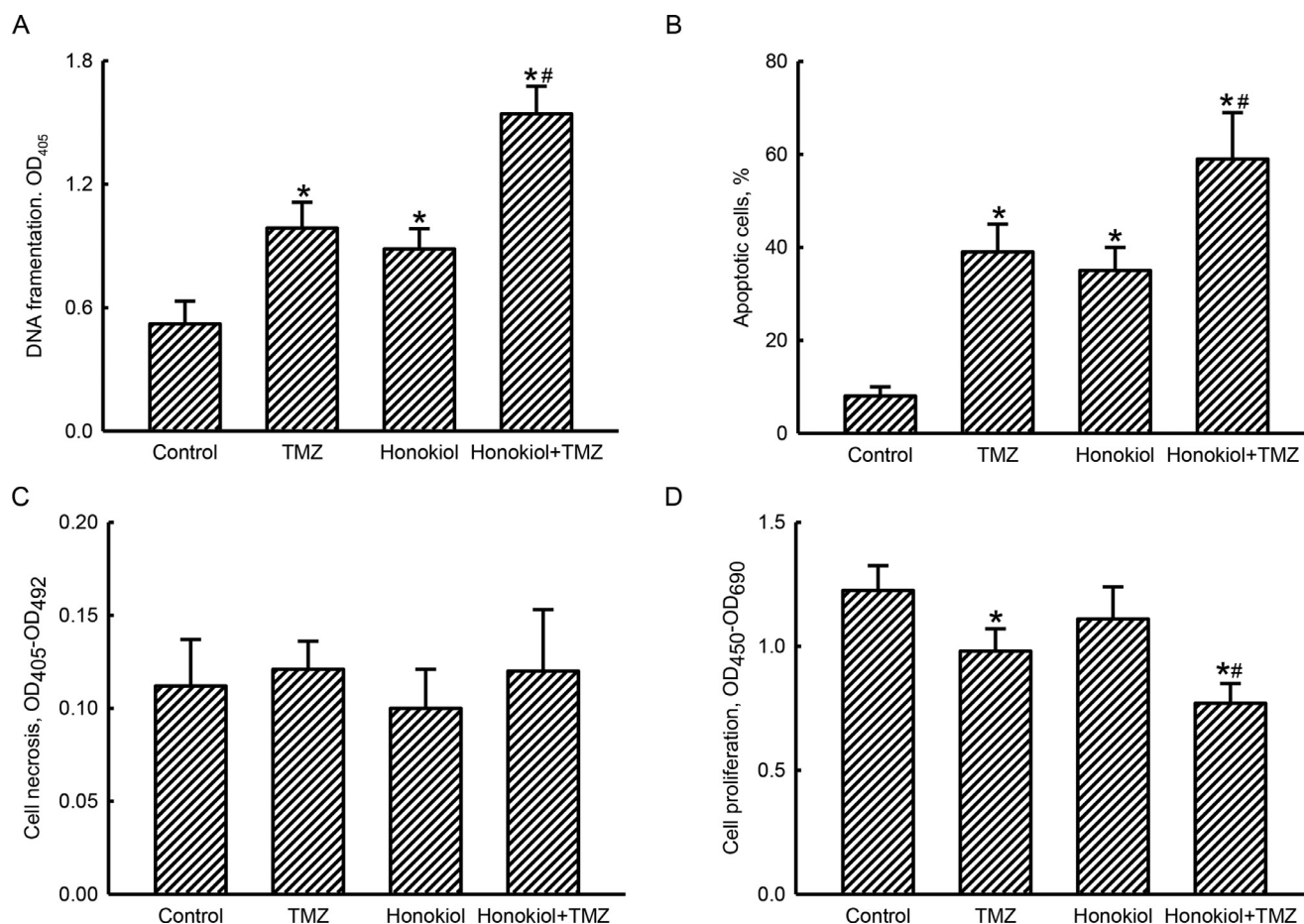


Fig. 2. Effects of honokiol on temozolomide (TMZ)-induced DNA fragmentation, apoptosis, necrosis, and proliferation of human glioma cells. Human U87 MG cells were exposed to 100 μ M TMZ, 40 μ M honokiol, and their combination for 72 h. DNA fragmentation was quantified with an ELISA (A). Cell apoptosis was measured with flow cytometry (B). Necrotic cells were quantified with a photometric immunoassay (C). A thymidine incorporation assay was carried out to determine the proliferation of human U87 MG cells (D). Each value represents the mean \pm SEM for $n = 6$. Symbols * and # indicate that the values significantly ($p < 0.05$) differed from the control and TMZ-treated groups, respectively.

(Fig. 2B). Cotreatment of honokiol and TMZ led to a 51% ($p = 0.025$) increase in TMZ-induced cell apoptosis. Remarkably, honokiol, TMZ, and combined treatment with these two drugs did not affect necrosis of human U87 MG cells (Fig. 2C). Proliferation of human glioma cells was repressed by 20% following TMZ administration for 72 h (Fig. 2D). Honokiol did not change proliferation of human U87 MG cells but caused a noteworthy 60% ($p = 0.003$) augmentation in TMZ-induced suppression of cell proliferation.

Honokiol specifically expands TMZ-induced apoptosis via an intrinsic pathway

Compared to untreated cells, exposure of human U87 MG cells to TMZ and honokiol alone for 72 h amplified caspase-9 activity by 3- and 2.8-fold, respectively (Fig. 3A). Cotreatment with honokiol and TMZ led to a significant 44% ($p = 0.016$) increase in caspase-9 activity in human glioma cells. Basal levels of caspase-8 activity were detected in human U87 MG cells (Fig. 3B). Exposure to TMZ for 72 h caused a slight 24% increase in caspase-8 activity. In contrast, honokiol did not influence basal or TMZ-induced activation of caspase-8 in human glioma cells (Fig. 3B). Levels of death Fas ligand were slightly enhanced in human U87 MG cells after TMZ treatment (Fig. 3C, top panel, lane 2). Honokiol did not change the basal or TMZ-induced augmentation in amounts of Fas ligand (Fig. 3C, lanes 3 and 4). GAPDH was immunodetected as the internal control (Fig. 3C, bottom panel). These protein bands were quantified and statistically analyzed (Fig. 3D). TMZ increased levels of

the Fas ligand by 84%. Honokiol did not affect TMZ-triggered augmentation in levels of this death ligand in human glioma cells ($p = 0.754$) (Fig. 3D).

Honokiol improves TMZ-induced augmentations in levels of apoptotic Bax and its translocation in human glioma cells

In untreated human U87 MG cells, basal levels of apoptotic Bax protein were detected (Fig. 4A, top panel, lane 1). After administration of TMZ and honokiol, amounts of Bax increased (Fig. 4A, lanes 2 and 3). In contrast, cotreatment with honokiol and TMZ elevated Bax expression in human glioma cells compared to the TMZ-treated group (lane 4). GAPDH was analyzed as the internal control (Fig. 4A, bottom panel). These protein bands were quantified and statistically analyzed (Fig. 4B). Exposure of human U87 MG cells to honokiol led to a 90% ($p = 0.002$) increase in TMZ-induced expression of apoptotic Bax protein.

Low levels of Bax were detected in the cytoplasm of untreated human U87 MG cells (Fig. 4C, top-left panel). After treatment with TMZ and honokiol, amounts of the cytosolic Bax protein had increased (Fig. 4C, top-middle panels). Compared to the TMZ-treated group, honokiol induced higher expression of Bax (Fig. 4C, top-right panel). Mitochondria and nuclei were recognized and labeled with DiOC₆ and DAPI (Fig. 4C, middle panels). Treatment of human U87 MG cells with TMZ and honokiol enhanced levels of the Bax protein colocalized with mitochondria (Fig. 4C, bottom panels). Honokiol enhanced TMZ-

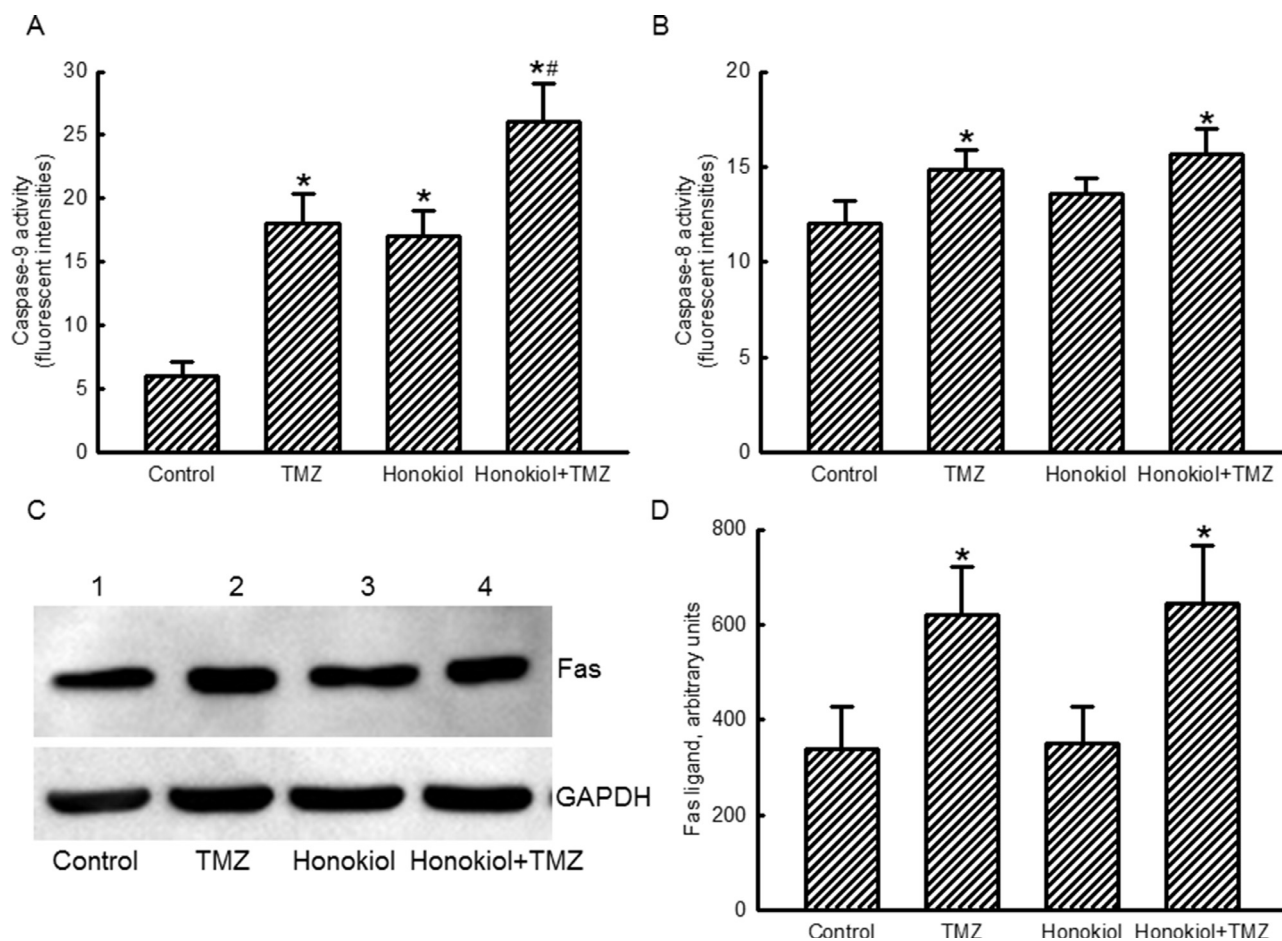


Fig. 3. Effects of honokiol on temozolomide (TMZ)-induced activation of caspases-8 and -9 and levels of the Fas ligand in human glioma cells. Human U87 MG cells were exposed to 100 μ M TMZ, 40 μ M honokiol, and their combination for 72 h. Activities of caspases-9 (A) and -8 (B) were assayed with fluorogenic substrate assays. Levels of the Fas ligand were immunodetected (C, top panel). GAPDH was analyzed as the internal control (bottom panel). Protein bands were quantified and statistically analyzed (D). Each value represents the mean \pm SEM for $n = 6$. Representative immunoblot images are shown. Symbols * and # indicate that the values significantly ($p < 0.05$) differed from the control and TMZ-treated groups, respectively.

induced translocation of Bax to mitochondria. The fluorescent intensities were quantified and statistically analyzed (Fig. 4D). Exposure to TMZ and honokiol respectively led to 3.8- and 3.2-fold increases in fluorescent intensities of Bax colocalized with mitochondria. Compared to the TMZ-treated group, cotreatment with honokiol significantly strengthened TMZ-induced Bax translocation by 2.1-fold ($p = 0.029$) (Fig. 4D).

Honokiol worsens TMZ-induced mitochondrial dysfunction in human glioma cells

Treatment of human U87 MG cells with TMZ for 72 h decreased the MMP by 16% (Fig. 5A). Honokiol alone did not change the MMP in human glioma cells. Nevertheless, cotreatment with honokiol induced a stronger TMZ-triggered reduction in the MMP by 25% ($p = 0.011$) (Fig. 5A). In parallel with a reduction in the MMP, exposure of human U87 MG cells to TMZ and honokiol alone respectively caused 2.5- and 2.7-fold augmentation in levels of intracellular ROS (Fig. 5B). In contrast, honokiol increased TMZ-induced elevation of levels of intracellular ROS by 87% ($p = 0.020$). Successively, treatment of human U87 MG cells with TMZ and honokiol respectively reduced mitochondrial complex I enzyme activities by 29% and 25% (Fig. 5C). Cotreatment with honokiol and TMZ enhanced TMZ-induced suppression of mitochondrial complex I enzyme activity in human glioma cells by 32% ($p = 0.004$) (Fig. 5C).

Honokiol improves TMZ-induced cytochrome c release and cascade activation of caspases-3 and -6

Compared to untreated cells, exposure of human U87 MG cells to TMZ and honokiol alone increased levels of cytochrome c (Fig. 6A, top panel, lanes 1–3). However, honokiol enhanced TMZ-induced elevation in amounts of cytochrome c in human glioma cells (Fig. 6A, lane 4). GAPDH was immunodetected as the internal control (bottom panel). These protein bands were quantified and statistically analyzed (Fig. 6B). Cotreatment with honokiol and TMZ caused a 59% ($p = 0.017$) augmentation in TMZ-induced release of cytochrome c in human U87 MG cells.

In parallel with growth of release of cytochrome c from mitochondria to the cytoplasm, exposure to TMZ and honokiol individually raised caspase-3 activities in human U87 MG cells by 77% and 91%, respectively (Fig. 6C). Simultaneously, activity of caspase-6 in human glioma cells were respectively elevated by 76% and 56% in human U87 MG cells (Fig. 6D). After cotreatment with honokiol and TMZ, the TMZ-induced augmentations in activities of caspases-3 and -6 were increased by 3.3- ($p = 0.021$) and 2.5-fold ($p = 0.030$), respectively (Fig. 6C and D).

Suppressing caspase-6 activity concurrently attenuates honokiol-involved enhancement of TMZ-induced apoptotic insults to human glioma cells

Exposure of human U87 MG cells to combined treatment with honokiol and TMZ caused a 2.8-fold increase in caspase-6 activity

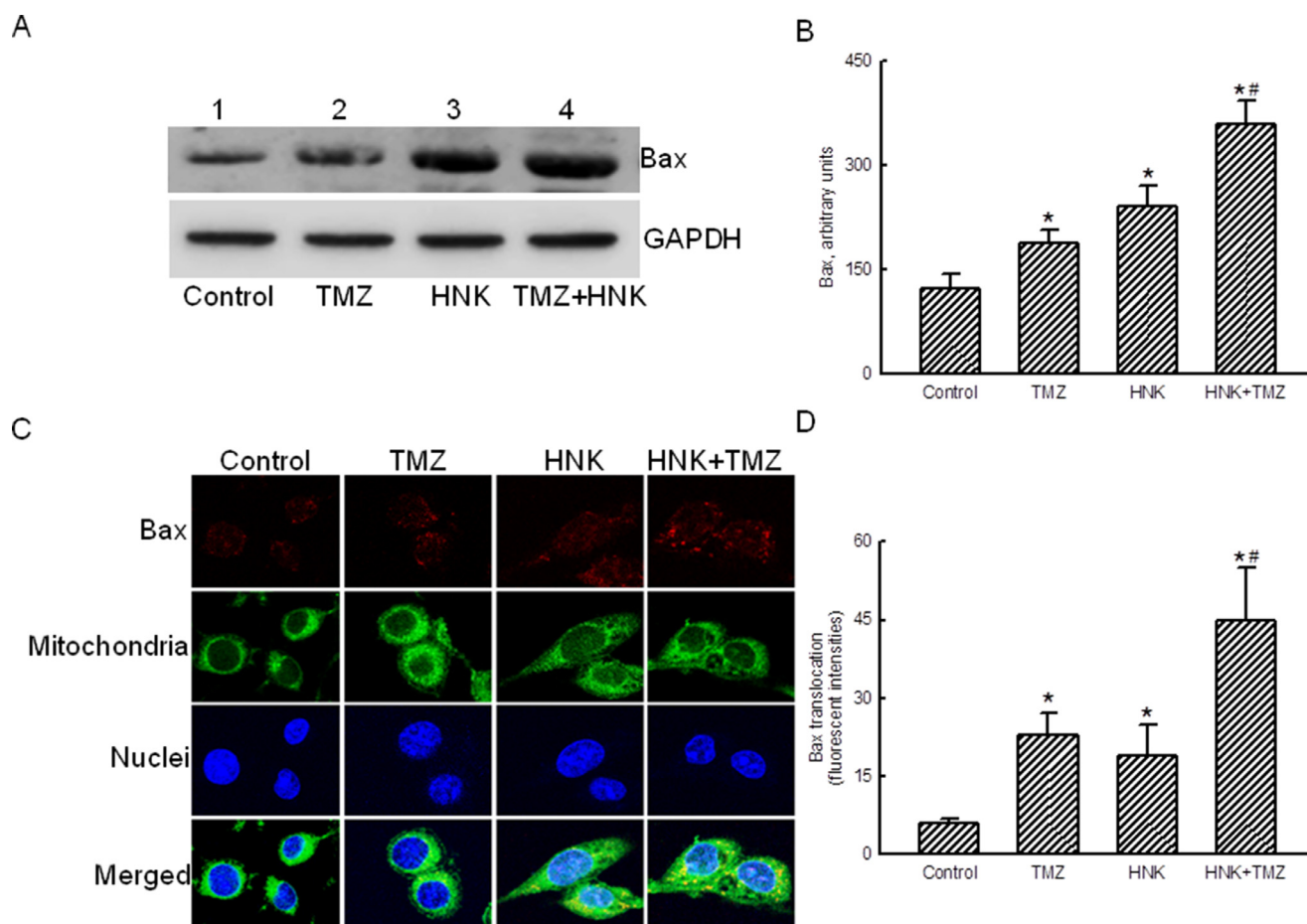


Fig. 4. Effects of honokiol on temozolomide (TMZ)-induced Bax expression and translocation in human glioma cells. Human U87 MG cells were exposed to 100 μ M TMZ, 40 μ M honokiol, and their combination for 72 h. Levels of Bax were immunodetected (A, top panel). GAPDH was analyzed as the internal control (bottom panel). Protein bands were quantified and statistically analyzed (B). The Bax protein in human U87 MG cells was immunodetected using an antibody with Cy3-conjugated streptavidin (C, top panels). Mitochondria and nuclei in human U87MG cells were respectively stained with DiOC₆ and DAPI (middle panels). The merged signals indicated that the Bax protein had been translocated into mitochondria (bottom panels). Merged fluorescent signals were quantified and statistically analyzed (D). Each value represents the mean \pm SEM for $n = 6$. Representative immunoblot images are shown. Symbols * and # indicate that the values significantly ($p < 0.05$) differed from the control and TMZ-treated groups, respectively.

(Fig. 7A). The honokiol-involved enhancement of TMZ-induced caspase-6 activation declined by 53%. Cotreatment of human U87 MG cells with honokiol and TMZ triggered DNA fragmentation by 160% and cell apoptosis by 61%, and decreased cell survival by 65% ($p = 0.001$) (Fig. 7B–D). Knocking down caspase-6 activation instantaneously alleviated honokiol-involved enhancement of TMZ-induced alterations of DNA fragmentation, cell apoptosis, and cell death by 49% ($p = 0.0033$), 63% ($p = 0.002$), and 49% ($p = 0.008$), respectively (Fig. 7B–D).

Honokiol-involved enhancement of TMZ-induced apoptotic insults was confirmed in human U373 MG and murine GL261 glioma cells

Exposure of human U373 MG cells and murine GL261 cells to TMZ and honokiol individually decreased cell survival (Table 1). Cotreatment with honokiol and TMZ enhanced TMZ-induced death of human and murine glioma cells. As to the mechanisms, treatment with honokiol specifically improved TMZ-induced activation of caspase-9 rather than caspase-8 (Table 1). Both honokiol and TMZ triggered apoptosis of human U373 MG and murine GL261 glioma cells. In contrast, treatment with honokiol enhanced TMZ-induced apoptosis of human and murine glioma cells by 70% ($p = 0.006$) and 65% ($p = 0.018$), respectively (Table 1).

Discussion

Honokiol can enhance TMZ-induced insults to malignant glioma cells. This study demonstrated that the LC₅₀ of honokiol to human U87 MG glioma cells was about 60 μ M. Herein, we further showed that honokiol at 40 μ M time-dependently changed cell morphology and decreased cell survival in human glioma cells. Our previous study showed that honokiol at 40 μ M was safe to normal brain cells, such as human astrocytes and cerebrovascular endothelia cells (Lin et al., 2012). Malignant gliomas are the most common and aggressive brain tumor (Saadatpour et al., 2016; Seano, 2018). Even though TMZ is a first-line chemotherapeutic drug for therapy of GBM patients, its side effects and drug resistance remain challenges and have limited its effectiveness to the present day (Omuro and DeAngelis, 2013). Thus, exploring *de novo* drugs that can overcome TMZ-induced side effects and drug resistance is very crucial. The present study showed enhanced effects of honokiol on TMZ-induced killing of human U87 MG cells. More interestingly, cotreatment of human glioma cells with honokiol decreased the concentration of TMZ which effectively led to the death of human glioma cells to 25 μ M. Lee et al. (2018) reported that metformin at a high dose increases TMZ-induced antitumor effects in glioblastoma *in vitro* and *in vivo*. In this study, we also showed that metformin at 10 mM could augment TMZ-induced apoptosis in

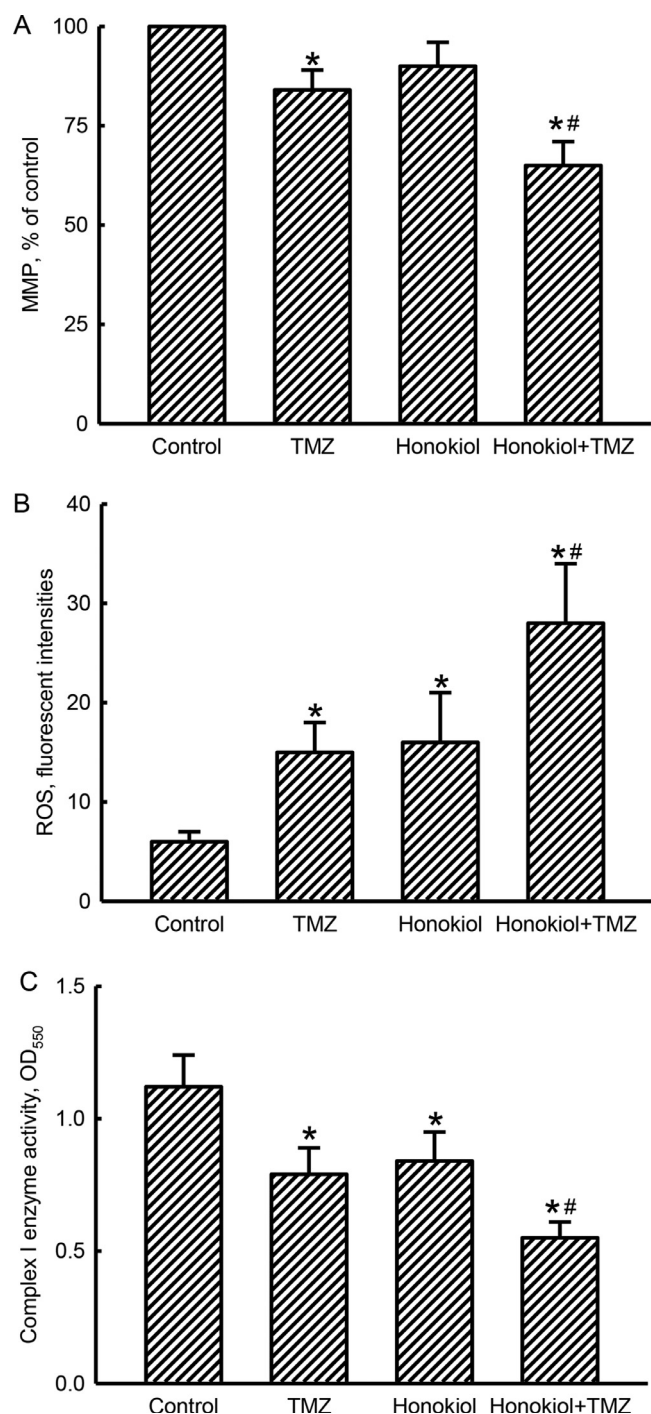


Fig. 5. Effects of honokiol on temozolomide (TMZ)-induced mitochondrial dysfunction in human glioma cells. Human U87 MG cells were exposed to 100 μ M TMZ, 40 μ M honokiol, and their combination for 72 h. The mitochondrial membrane potential (MMP) was quantified by flow cytometry (A). Levels of intracellular reactive oxygen species (ROS) were measured by flow cytometry (B). The activity of mitochondrial complex I was assayed with a colorimetric method (C). Each value represents the mean \pm SEM for $n = 6$. Symbols * and # indicate that the values significantly ($p < 0.05$) differed from the control and TMZ-treated groups, respectively.

human glioma cells (data not shown). In addition, the honokiol-involved enhancement of TMZ-induced killing of malignant glioma cells was further confirmed in human U373 MG and murine GL261 cells. U373 MG cells and GL261 cells are respectively derived from human and mouse glioblastomas-astrocytomas (Prat et al., 2000; Szatmári

et al., 2006). Our previous studies proved toxic effects of honokiol to brain tumor cells (Lin et al., 2012, 2016a,b; Chio et al., 2018). According to the Loewe additive model, the combination of honokiol and TMZ showed additive cytotoxicity to human glioma cells. This study showed the potential of honokiol to decrease TMZ-induced side effects.

Honokiol enhances TMZ-induced insults to human malignant glioma cells via an apoptotic mechanism. Our results revealed that exposure to honokiol led to significant augmentation in TMZ-induced shrunken morphology in human glioma cells. In parallel, TMZ-induced DNA fragmentation and cell cycle arrest at the subG₁ phase significantly increased. A shrunken morphology, DNA fragmentation, and cell cycle arrest at the subG₁ phase are typical features indicating that cells are undergoing apoptosis (Goyal, 2001; Aubrey et al., 2018). A photometric immunoassay further showed that neither honokiol, TMZ, nor combined treatment triggered cell necrosis. Hence, honokiol can precisely improve TMZ-induced insults toward human glioma cells via an apoptotic mechanism. Our thymidine incorporation assay proved the enhancement by honokiol of TMZ-induced suppression of cell proliferation in human U87 MG cells. The 5-year survival rate of GBM is only 5% (Daher and de Groot, 2018). Uncontrolled tumor proliferation is one of critical reasons explaining the poor outcomes of GBM patients (Staudacher et al., 2014). Therefore, honokiol can possibly be clinically applied to expand therapeutic effects of TMZ towards malignant gliomas through specifically triggering cell apoptosis and suppressing cell proliferation.

Honokiol enhances TMZ-induced apoptosis of malignant glioma cells via an intrinsic pathway. An extrinsic apoptosis mechanism is originated by activating the Fas ligand and death Fas receptor (Bao and Shi, 2007). The present results disclosed that cotreatment of human U87 MG cells with honokiol did not change TMZ-induced alteration of levels of the Fas ligand. In addition, activation of caspase-8 is another important indicator explaining extrinsic apoptosis (Fulda, 2015). Honokiol did not influence TMZ-induced caspase-8 activation in human glioma cells. Instead, TMZ-induced promotion of caspase-9 activity obviously increased following honokiol administration. Caspase-9 can be considered a noteworthy initiator protease elucidating intrinsic apoptosis (Li et al., 2017). Thus, the honokiol-involved augmentation of TMZ-induced apoptosis mainly occurs through an intrinsic apoptotic pathway. Caspase-9 activation, involved in the homo-dimerization of monomeric zymogens and binding to the apoptosome, can induce considerable catalytic activity for downstream caspases (Bao and Shi, 2007). Recently, Kim et al. suggested that caspase-9 can be a therapeutic target for treating various cancers (Kim et al., 2015). Therefore, honokiol may enhance TMZ-induced apoptotic insults to human glioma cells by activating caspase-9 protease activity.

Bax translocation and subsequent mitochondrial dysfunction are involved in the honokiol-induced enhancement of cell apoptosis. Bax, a member of the B-cell leukemia/lymphoma 2 (Bcl-2) family, is a pro-apoptotic protein that functions to permeabilize the outer membrane of mitochondria following translocation from the cytoplasm and interactions with the antiapoptotic Bcl-2 and Bcl-X_L proteins (Karch and Molkenin, 2015). Herein, we showed the enhanced effects of honokiol on TMZ-induced augmentations in levels of cellular Bax. Such an increase leads to a decrease in the ratio of Bcl-2 over Bax, driving Bax translocation and cellular apoptosis. Our results demonstrated honokiol-induced translocation of Bax from the cytoplasm to mitochondrial outer membranes. The honokiol-induced diminution in the MMP is due to Bax-involved permeabilization of the mitochondrial membrane. Successively, honokiol enhanced TMZ-induced changes in intracellular ROS levels and the MMP. Disruption of the MMP can lead to mitochondrial dysfunction (Franklin, 2011; Chang et al., 2016). Taken together, honokiol can improve TMZ-induced Bax translocation and mitochondrial dysfunction and then triggers more apoptotic insults to human glioma cells.

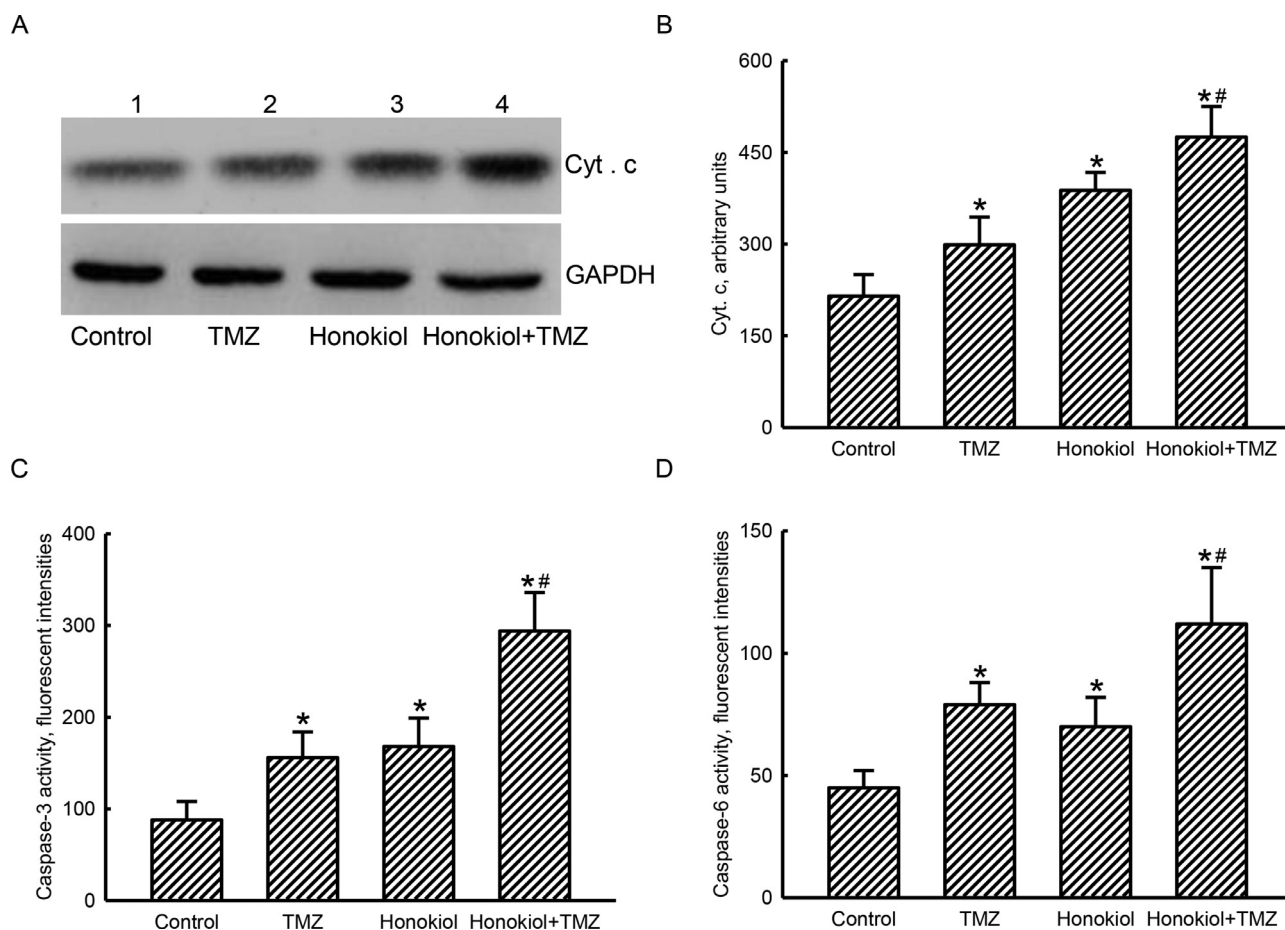


Fig. 6. Effects of honokiol on temozolomide (TMZ)-induced release of cytochrome (Cyt) c and cascade activation of caspases-3 and -6 in human glioma cells. Human U87 MG cells were exposed to 100 μ M TMZ, 40 μ M honokiol, and their combination for 72 h. Levels of Cyt c were immunodetected (A, top panel). GAPDH was analyzed as the internal control (bottom panel). Protein bands were quantified and statistically analyzed (B). Activities of caspases-3 (C) and -6 (D) were assayed with fluorogenic substrate methods. Each value represents the mean \pm SEM for $n = 6$. Representative immunoblot images are shown. Symbols * and # indicate that the values significantly ($p < 0.05$) differed from the control and TMZ-treated groups, respectively.

Honokiol sequentially induces release of cytochrome *c* and cascade activation, thereby augmenting TMZ-induced cell apoptosis. In parallel with Bax translocation and MMP reduction, levels of cytochrome *c* in human glioma cells consecutively increased after cotreatment with honokiol and TMZ. Cytochrome *c*, a small hemoprotein loosely localized in inner membranes of mitochondria, participates in the electron transport chain (Alvarez-Paggi et al., 2017). Park et al. (2012) reported that blockage of mitochondrial Bax translocation simultaneously attenuates mitochondrial dysfunction and cytochrome *c* release and protects against prion peptide-induced neuronal death. Thus, honokiol-induced enhancement of cytochrome *c* release in human glioma cells is due to Bax translocation and mitochondrial dysfunction. Cytochrome *c* released from mitochondria to the cytoplasm can react with apoptotic protease-activating factor (Apaf-1 and the apoptosome to form a complex with the assistance of deoxyadenosine triphosphate (Jiang and Wang, 2000). The multimeric cytochrome *c*-Apaf-1 complex then triggers procaspase-9 into its activated form (Ow et al., 2008). This study showed that honokiol raised TMZ-induced enhancement of caspase-9 protease activity in human glioma cells via elevation of cytochrome *c* release from mitochondria. Activation of caspase-9 induces cascade initiation of caspases-6 and -3 (Ow et al., 2008). After being sequentially activated, cleaved caspases-3 and -6 may degrade key cellular proteins, such as lamin and nuclear mitotic apparatus proteins, to affect cell activity and function (Rao et al., 1996). Consecutive TMZ-induced increases in activities of caspases-3 and -6 in human glioma cells were

augmented by honokiol treatment. Interestingly, suppressing caspase-6 activity simultaneously downregulated the honokiol-induced enhancement. Therefore, cascade activation of caspase-9, -3, and -6 contributes to honokiol-involved enhancement of TMZ-induced apoptosis in human glioma cells.

In summary, this study showed that honokiol can enhance TMZ-induced apoptotic insults to human U87 MG and U373 MG cells and murine GL261 glioma cells. As to the mechanisms, the honokiol-involved enhancement of TMZ-induced apoptosis of human glioma cells took place via an intrinsic pathway. Subsequently, TMZ-induced Bax translocation and mitochondrial dysfunction were augmented by honokiol. Cytochrome *c* release and cascade activation of caspase-9, -3, and -6 in TMZ-treated human glioma cells consequently increased following honokiol administration. Therefore, honokiol can improve TMZ-induced apoptosis of glioma cells via an intrinsic Bax/mitochondria/Cyt *c*/caspase proteinase activation mechanism. Honokiol has the potential to be clinically applied to reduce TMZ-induced side effects and drug resistance.

Conflict of interest

We wish to confirm that there are no known conflicts of interest associated with this publication and there has been no significant financial support for this work that could have influenced its outcome.

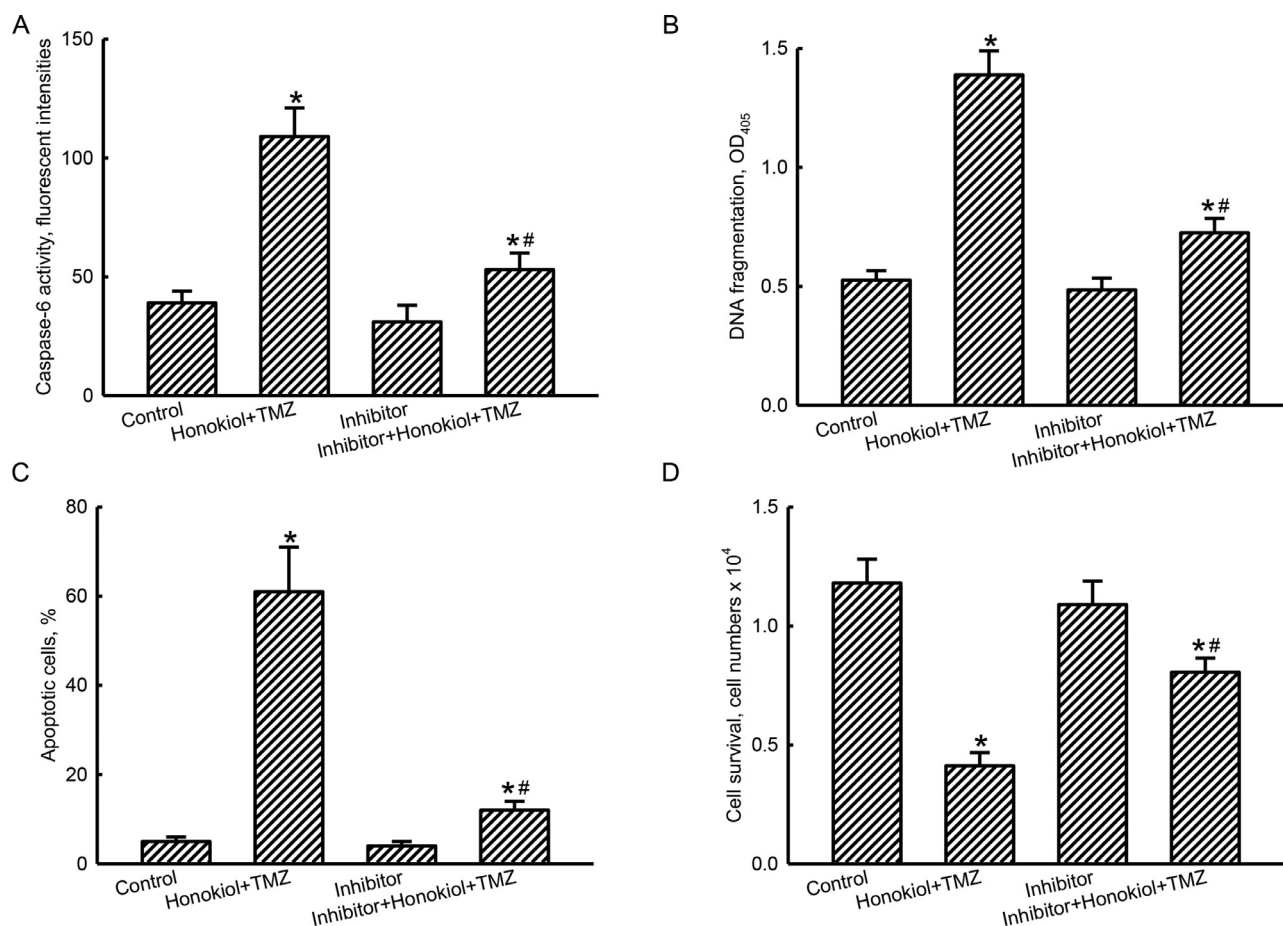


Fig. 7. Roles of caspase-6 in honokiol-involved enhancement of temozolomide (TMZ)-induced DNA fragmentation, cell apoptosis, and cell survival in human glioma cells. Human U87MG cells were pretreated with a caspase-6 peptide inhibitor (inhibitor) for 1 h and then exposed to a combination of honokiol and TMZ for another 72 h. The activity of caspase-6 was assayed with fluorogenic substrate methods. Caspase-6 activity was measured (C). Apoptotic cells were quantified with flow cytometry (D). Each value represents the mean \pm SEM from six independent experiments. Symbols * and # indicate that the values significantly ($p < 0.05$) differed from the control and TMZ-treated groups, respectively.

Table 1

Effects of temozolomide (TMZ), honokiol (HNK), and their combined treatment on cell survival, caspase-8 activity, caspase-9 activity, and apoptosis of human U373 MG and murine GL261 glioma cells.

	Control	TMZ	HNK	HNK + TMZ
U373 MG Cells				
Cell survival (%)	100	59 \pm 9*	66 \pm 11*	39 \pm 4**
Caspase-8 activity (FI)	13 \pm 2	18 \pm 2*	17 \pm 3	21 \pm 4*
Caspase-9 activity (FI)	7 \pm 1	17 \pm 3*	18 \pm 4*	33 \pm 9**
Apoptotic cells (%)	5 \pm 1	30 \pm 6*	24 \pm 4*	51 \pm 7**
GL261 Cells				
Cell survival (%)	100	63 \pm 12*	72 \pm 14*	48 \pm 5**
Caspase-8 activity (FI)	12 \pm 3	16 \pm 3	17 \pm 4	20 \pm 3*
Caspase-9 activity (FI)	6 \pm 1	14 \pm 3*	15 \pm 4*	26 \pm 5**
Apoptotic cells (%)	4 \pm 1	26 \pm 4*	23 \pm 5*	43 \pm 9**

Human U373 MG and murine GL261 glioma cells were treated with TMZ (100 μ M), HNK (40 μ M), and their combination for 72 h. Cell survival was analyzed with a trypan blue exclusion method. Activities of caspases-8 and -9 were examined with fluorometric substrate assays, and results are reported in fluorescent intensity (FI). Apoptotic cells were quantified using flow cytometry. Each value represents the mean \pm SEM for $n = 6$. Symbols * and # indicate that the values significantly ($p < 0.05$) differed from the control and TMZ-treated groups, respectively.

Acknowledgments

This study was supported by grants from Chi-Mei Medical Center (104CM-TMU-16-1), Wan-Fang Hospital (106swf04), and Featured Areas Research Center Program within the framework of the Higher Education Sprout Project by the Ministry of Education, Taipei, Taiwan. The authors appreciate the assistance from Dr. Robbin Lin, Research Center of Biostatistics, College of Management, Taipei Medical University, Taipei Taiwan, for statistical analyses.

References

- Alvarez-Paggi, D., Hannibal, L., Castro, M.A., Oviedo-Rouco, S., Demicheli, V., Tortora, V., Tomasina, F., Radi, R., Murgida, D.H., 2017. Multifunctional cytochrome c: learning new tricks from an old dog. *Chem. Rev.* 117, 13382–13460.
- Aubrey, B.J., Kelly, G.L., Janic, A., Herold, M.J., Strasser, A., 2018. How does p53 induce apoptosis and how does this relate to p53-mediated tumour suppression? *Cell Death Differ.* 25, 104–113.
- Bao, Q., Shi, Y., 2007. Apoptosome: a platform for the activation of initiator caspases. *Cell Death Differ.* 14, 56–65.
- Bilia, A.R., Piazzini, V., Guccione, C., Risaliti, L., Asprea, M., Capecchi, G., Bergonzi, M.C., 2017. Improving on nature: the role of nanomedicine in the development of clinical natural drugs. *Planta Med.* 83, 366–381.
- Bonner, M.Y., Karlsson, I., Rodolfo, M., Arnold, R.S., Vergani, E., Arbiser, J.L., 2016. Honokiol bis-dichloroacetate (Honokiol DCA) demonstrates activity in vemurafenib-resistant melanoma *in vivo*. *Oncotarget* 7, 12857–12868.
- Chang, C.Y., Lui, T.N., Lin, J.W., Lin, Y.L., Hsing, C.H., Wang, J.J., Chen, R.M., 2016.

- Roles of microRNA-1 in hypoxia-induced apoptotic insults to neural cells. *Arch. Toxicol.* 90, 191–202.
- Chen, R.M., Tai, Y.T., Chen, T.G., Lin, T.H., Chang, H.C., Chen, T.L., Wu, G.J., 2013. Propofol protects against nitrosative stress-induced breakage of the blood-brain barrier through reducing apoptotic insults to cerebrovascular endothelial cells. *Surgery* 154, 58–68.
- Cheng, B.C., Chen, J.T., Yang, S.T., Chio, C.C., Liu, S.H., Chen, R.M., 2017. Cobalt chloride treatment induces autophagic apoptosis in human glioma cells via a p53-dependent pathway. *Int. J. Oncol.* 50, 964–974.
- Chio, C.C., Chen, K.Y., Chuang, J.Y., Liu, C.C., Liu, S.H., Chen, R.M., 2018. Improved effects of honokiol on temozolomide-induced autophagy and apoptosis of drug-sensitive and -tolerant glioma cells. *BMC Cancer* 18, 379.
- Chio, C.C., Lin, J.W., Cheng, H.A., Chiu, W.T., Wang, Y.H., Wang, J.J., Hsing, C.H., Chen, R.M., 2013. MicroRNA-210 targets antiapoptotic Bcl-2 expression and mediates hypoxia-induced apoptosis of neuroblastoma cells. *Arch. Toxicol.* 87, 458–468.
- Chio, C.C., Wei, L., Chen, T.G., Tsai, S.H., Shieh, J.P., Yeh, P.S., Chen, R.M., 2016. Neuron-derived orphan receptor 1 transduces survival signals in neuronal cells in response to hypoxia-induced apoptotic insults. *J. Neurosurg.* 124, 1654–1664.
- Chuang, C.Y., Chen, T.L., Cheng, Y.G., Tai, Y.T., Chen, T.G., Chen, R.M., 2011. Lipopolysaccharide induces apoptotic insults to human alveolar epithelial A549 cells through reactive oxygen species-mediated activation of an intrinsic mitochondrion-dependent pathway. *Arch. Toxicol.* 85, 209–218.
- Daher, A., de Groot, J., 2018. Rapid identification and validation of novel targeted approaches for Glioblastoma: a combined ex vivo-in vivo pharmaco-omic model. *Exp. Neurol.* 299, 281–288.
- Franklin, J.L., 2011. Redox regulation of the intrinsic pathway in neuronal apoptosis. *Antioxid. Redox. Signal.* 14, 1437–1448.
- Fried, L.E., Arbiser, J.L., 2009. Honokiol, a multifunctional antiangiogenic and antitumor agent. *Antioxid. Redox. Signal.* 11, 1139–1148.
- Fulda, S., 2015. Targeting extrinsic apoptosis in cancer: challenges and opportunities. *Semin. Cell. Dev. Biol.* 39, 20–25.
- Furnari, F.B., Cloughesy, T.F., Cavenee, W.K., Mischel, P.S., 2015. Heterogeneity of epidermal growth factor receptor signalling networks in glioblastoma. *Nat. Rev. Cancer* 15, 302–310.
- Goyal, L., 2001. Cell death inhibition: keeping caspases in check. *Cell* 104, 805–808.
- Hahn, E.R., Arlotti, J.A., Marynowski, S.W., Singh, S.V., 2008. Honokiol, a constituent of oriental medicinal herb *magnolia officinalis*, inhibits growth of PC-3 xenografts *in vivo* in association with apoptosis induction. *Clin. Cancer Res.* 14, 1248–1257.
- Ho, M.H., Liao, M.H., Lin, Y.L., Lai, C.H., Lin, P.I., Chen, R.M., 2014. Improving effects of chitosan nanofiber scaffolds on osteoblast proliferation and maturation. *Int. J. Nanomed.* 9, 4293–4304.
- Hottinger, A.F., Pacheco, P., Stupp, R., 2016. Tumor treating fields: a novel treatment modality and its use in brain tumors. *Neuro-Oncol* 18, 1338–1349.
- Jiang, X., Wang, X., 2000. Cytochrome c promotes caspase-9 activation by inducing nucleotide binding to Apaf-1. *J. Biol. Chem.* 275, 31199–31203.
- Karch, J., Molkenin, J.D., 2015. Regulated necrotic cell death: the passive aggressive side of Bax and Bak. *Circ. Res.* 116, 800–1809.
- Kim, B., Srivastava, S.K., Kim, S.H., 2015. Caspase-9 as a therapeutic target for treating cancer. *Expert Opin. Ther. Targets* 19, 113–127.
- Lee, J.E., Lim, J.H., Hong, Y.K., Yang, S.H., 2018. High-dose metformin plus temozolomide shows increased anti-tumor effects in glioblastoma *in vitro* and *in vivo* compared with monotherapy. *Cancer Res. Treat.* <https://doi.org/10.4143/crt.2017.466>.
- Li, P., Zhou, L., Zhao, T., Liu, X., Zhang, P., Liu, Y., Zheng, X., Li, Q., 2017. Caspase-9: structure, mechanisms and clinical application. *Oncotarget* 8, 23996–24008.
- Lin, C.J., Chang, Y.A., Lin, Y.L., Chio, C.C., Chen, R.M., 2016a. Preclinical effects of honokiol on treating glioblastoma multiforme via G1 phase arrest and cell apoptosis. *Phytomedicine* 23, 517–527.
- Lin, C.J., Chen, T.L., Tseng, Y.Y., Wu, G.J., Hsieh, M.H., Lin, J.W., Chen, R.M., 2016b. Honokiol induces autophagic cell death in malignant glioma through reactive oxygen species-mediated regulation of the p53/PI3K/Akt/mTOR signaling pathway. *Toxicol. Appl. Pharmacol.* 304, 59–69.
- Lin, J.W., Chen, J.T., Hong, C.Y., Lin, Y.L., Wang, K.T., Yao, C.J., Lai, G.M., Chen, R.M., 2012. Honokiol traverses the blood-brain barrier and induces apoptosis of neuroblastoma cells via an intrinsic bax-mitochondrion-cytochrome c-caspase protease pathway. *Neuro-Oncol* 14, 302–314.
- Lin, P.I., Tai, Y.T., Chan, W.P., Lin, Y.L., Liao, M.H., Chen, R.M., 2018. Estrogen/ER α signaling axis participates in osteoblast maturation via upregulating chromosomal and mitochondrial complex gene expressions. *Oncotarget.* <https://doi.org/10.18632/oncotarget.23453>.
- Lo, Y.C., Teng, C.M., Chen, C.F., Chen, C.C., Hong, C.Y., 1994. Magnolol and honokiol isolated from *Magnolia officinalis* protect rat heart mitochondria against lipid peroxidation. *Biochem. Pharmacol.* 47, 549–553.
- Mills, C.C., Kolb, E.A., Sampson, V.B., 2018. Development of chemotherapy with cell-cycle inhibitors for adult and pediatric cancer therapy. *Cancer Res.* <https://doi.org/10.1158/0008-5472.CAN-17-2782>.
- Omuro, A., DeAngelis, L.M., 2013. Glioblastoma and other malignant gliomas: a clinical review. *JAMA* 310, 1842–1850.
- Ow, Y.P., Green, D.R., Hao, Z., Mak, T.W., 2008. Cytochrome c: functions beyond re-spiration. *Nat. Rev. Mol. Cell. Biol.* 9, 532–542.
- Ooko, E., Kadioglu, O., Greten, H.J., Efferth, T., 2017. Pharmacogenomic characterization and isobologram analysis of the combination of ascorbic acid and curcumin-two main metabolites of *curcuma longa*-in cancer cells. *Front. Pharmacol.* 8, 38.
- Pan, J., Lee, Y., Wang, Y., You, M., 2016. Honokiol targets mitochondria to halt cancer progression and metastasis. *Mol. Nutr. Food Res.* 60, 1383–1395.
- Park, Y.G., Jeong, J.K., Moon, M.H., Lee, J.H., Lee, Y.J., Seol, J.W., Kim, S.J., Kang, S.J., Park, S.Y., 2012. Insulin-like growth factor-1 protects against prion peptide-induced cell death in neuronal cells via inhibition of Bax translocation. *Int. J. Mol. Med.* 30, 1069–1074.
- Prat, E., Baron, P., Meda, L., Scarpini, E., Galimberti, D., Ardolino, G., Catania, A., Scarlato, G., 2000. The human astrocytoma cell line U373MG produces monocyte chemotactic protein (MCP)-1 upon stimulation with beta-amyloid protein. *Neurosci. Lett.* 283, 177–180.
- Rao, L., Perez, D., White, E., 1996. Lamin proteolysis facilitates nuclear events during apoptosis. *J. Cell. Biol.* 135, 1441–1455.
- Saadatpour, L., Fadaee, E., Fadaei, S., Nassiri Mansour, R., Mohammadi, M., Mousavi, S.M., Goodarzi, M., Verdi, J., Mirzaei, H., 2016. Glioblastoma: exosome and microRNA as novel diagnosis biomarkers. *Cancer Gene Ther.* 23, 415–418.
- Seano, G., 2018. Targeting the perivascular niche in brain tumors. *Curr. Opin. Oncol.* 30, 54–60.
- Staudacher, I., Jehle, J., Staudacher, K., Pledl, H.W., Lemke, D., Schweizer, P.A., Becker, R., Katus, H.A., Thomas, D., 2014. HERG K⁺ channel-dependent apoptosis and cell cycle arrest in human glioblastoma cells. *PLoS One* 9, e88164.
- Szatmári, T., Lumnitzky, K., Désaknai, S., Trajcevski, S., Hídvégi, E.J., Hamada, H., Sáfrány, G., 2006. Detailed characterization of the mouse glioma 261 tumor model for experimental glioblastoma therapy. *Cancer Sci.* 97, 546–553.
- Wu, G.J., Chen, J.T., Tsai, H.C., Chen, T.L., Liu, S.H., Chen, R.M., 2017. Protection of dexmedetomidine against ischemia/reperfusion-induced apoptotic insults to neuronal cells occurs via an intrinsic mitochondria-dependent pathway. *J. Cell. Biochem.* 118, 2635–2644.
- Wu, G.J., Wang, W., Lin, Y.L., Liu, S.H., Chen, R.M., 2016. Oxidative stress-induced apoptotic insults to rat osteoblasts are attenuated by nitric oxide pretreatment via GATA-5-involved regulation of Bcl-X_L gene expression and protein translocation. *Arch. Toxicol.* 90, 905–916.
- Yeh, P.S., Wang, W., Chang, Y.A., Lin, C.J., Wang, J.J., Chen, R.M., 2016. Honokiol induces autophagy of neuroblastoma cells through activating the PI3K/Akt/mTOR and endoplasmic reticular stress/ERK1/2 signaling pathways and suppressing cell migration. *Cancer Lett.* 370, 66–77.